Supporting Information

Rosenbluth et al. 10.1073/pnas.1011936108

SI Materials and Methods

Cell Culture and Treatment. Rh30, Rh28, Rh41, and Rh1 (from P. Houghton, St. Jude Hospital, Memphis, TN) and H1299 cells were cultured, and rapamycin (Calbiochem) was used in serum-free media as previously described (1). Human MSCs were obtained from ScienCell and maintained according to the manufacturer's recommendations, or were isolated from human joint tissue at Vanderbilt University with Institutional Review Board approval. MSCs were treated with 5AZA (Sigma) for 8 to 24 h as previously described (2). Human keratinocytes were maintained as previously described (3). ME180 cells (from K. Cho, University of Michigan, Ann Arbor, MI) were maintained in DMEM.

RNA Isolation, Expression Arrays, and Statistical Analyses. RNA was isolated from MSCs and qRT-PCR performed as previously described (1). Microarray experiments were performed in duplicate in Rh30 cells treated as above, and RNA was isolated using the Aurum total RNA minikit (Bio-Rad) and submitted to the Vanderbilt-Ingram Cancer Center Functional Genomics Shared Resource for quality control. The RNA was processed, and Affymetrix Hu Gene 1.0 ST microarrays were hybridized as previously described and according to Functional Genomics Shared Resource/Affymetrix protocols (1).

Cell Transfection/Infection and shRNA. The following sequences were used for RNAi: p73-1, 5′-GCAATAATCTCTCGCAGTA-3′, p73-2, 5′-GAACCAGACAGCACCTACT-3′, p73-3, 5′-GGATTCC-AGCATGGACGTC-3′, and GFP, 5′-GAAGGTGATACCCTT-GTTA-3′. The 293T cells were transfected using Fugene 6 (Roche) for viral production. For knockdown of p73, the pSicoR lentivirus system was used. Production of virus and transduction were performed as previously described (1). H1299 cells were infected with adenovirus expressing hemagglutinin-TAp73β (pAdEasy-1:HA-TAp73β), as previously described (1). The pAdEasy was provided by B. Vogelstein (Johns Hopkins Medicine, Baltimore). For knockdown of c-Jun, Rh30 cells were transfected with Dharmacon OnTarget plus smartpool siRNA for Jun (J-003268-10, -11, -12 and -13) using Dharmafect 1 lipid according to the manufacturer's directions.

Protein Lysate Preparation and Western Analysis. For analysis of protein levels in ChIP-on-Chip duplicate samples, fixed cells were resuspended in cell lysis buffer and dounce-homogenized as previously described (4). Nuclear pellets were resuspended in sonication buffer and Western analysis was performed as previously described (1) on a chromatin-enriched fraction. For analysis of siJun and siControl samples, cells were lysed in RIPA buffer and Western analysis was performed as previously described (1). The following antibodies were used: p73 antibodies IMG-246 and IMG-259 (Imgenex), c-Jun 9168 antibody (Cell Signaling Technology), phospho-S6 Ser235/236 polyclonal antibody 2F9, total S6 monoclonal antibody 54D2 (Cell Signaling Technology), and β-actin polyclonal antibody I-19 (Santa Cruz Biotechnology).

MicroRNA Isolation and Expression Analysis. MicroRNA analyses were performed as follows: Rh30 cells were treated with vehicle or 40 nM rapamycin for 24 h after infection with lentivirus-expressing shRNA targeting GFP or TAp73 for 3 d, and RNA was isolated using the miRVana minikit (Applied Biosystems). Duplicate samples were sent to the Vanderbilt-Ingram Cancer Center Functional Genomics Shared Resource for quality control. The RNA was reverse transcribed, and cDNA hybridized to TaqMan Low Density Array version 2.0 cards A and B without preamplification for MultiPlex qRT-PCR analysis, according to the manufacturer's instructions (Applied Biosystems). Data were analyzed and normalized using the ΔΔCT method, by averaging sample values from two independent experiments. MicroRNAs with low copy number (CT > 35) were excluded.

For miR-133b and RNU19 qRT-PCR analysis, RNA samples from three independent experiments were harvested as above, reverse transcription was performed using the TaqMan Reverse Transcription kit, and real-time PCR was performed using the TaqMan MicroRNA Assays according to the manufacturer's instructions (Applied Biosystems).

Microarray Statistical Analyses and Locations of Publicly Available Datasets. Samples were generated using Rh30 cells treated with rapamycin, and with p73 knock-down using the pSicoR system (5), as described in the main text. Probe summarization algorithms, similar to those described elsewhere (1), were used to identify changes in transcript expression levels. Expression levels have been log-transformed. GeneSpring GX software (Agilent) was used for statistical analyses and transcript annotations, and for algorithms involved in hierarchical clustering, Venn analysis, classification, box plots, bar charts, statistical similarity of gene lists, and Benjamini-Hochberg multiple testing-corrected *t*- and ANOVA testing. Probe-level analyses were performed with microarray data, and probes were converted to genes for cross-comparison with ChIP data.

Publicly available datasets were obtained from various locations as follows: The Wachtel et al. (6) and Davicioni et al. (7) rhabdomyosarcoma datasets are based on Affymetrix chips (HG-U133A) and are available at the EBI ArrayExpress database (E-MEXP-121) and the National Cancer Institute Cancer Array Database (trich-00099), respectively. Mesenchymal stem cell data were obtained from the National Center for Biotechnology Information Gene Expression Omnibus under the accession number GSE9764.

Analysis of p73 Protein Levels and Mammalian Target of Rapamycin Activity in Rhabdomyosarcomas. Analyses of the p73 gene signature were performed using microarray data derived from the rhabdomyosarcoma samples described in the section above. Expression of p73 protein and mammalian target of rapamycin (mTOR) activity was assessed using immunohistochemical analysis of p73 [two separate analyses were performed with antibodies: IHC-00197 (Bethyl) and H-79 (Santa Cruz Biotechnology)] and phospho-S6 [Ser235/236, 91B2 (Cell Signaling)] using paraffin-embedded sections of rhabdomysarcoma specimens kindly provided by Cheryl Coffin in the Vanderbilt Department of Pathology, Nashville, TN (protocols available upon request). C. Coffin is internationally recognized for her expertise in pediatric surgical and soft tissue pathology. The p73 and phospho-S6 staining were detected in 60% of the samples, confirming that p73 protein is expressed and mTOR is active (using phospho-S6 staining as a surrogate marker) in human rhabdomyosarcomas, respectively.

ChIP, ChIP-on-Chip, the FactorPath Protocol, and Statistical Analyses. The following antibodies were used for immunoprecipitation of p73-DNA complexes: anti-TAp73 A300-126A (Bethyl), which recognizes an epitope within amino acids 1 to 62 of TAp73 isoforms; anti-TAp73 H-79 (Santa Cruz), which recognizes an epitope within amino acids 1 to 80 of TAp73 isoforms; anti-p73α ER-13 (Ab-1; Calbiochem), which recognizes an epitope within amino

acids 495 to 637 that is unique to p73α; and anti-p73β GC-15 (Ab-3, Calbiochem), which recognizes an epitope in amino acids 380 to 499 that is unique to p73β. Antibody specificity was confirmed using cells in which different p73 isoforms had been overexpressed, as previously described (1).

For ChIP-qPCR, primer sequences are available upon request. For ChIP-on-Chip, probe signal and enrichment analysis was performed using Affymetrix Tiling Analysis Software. An estimate of fold-enrichment was obtained by computing the ratio of signal for each probe on the ChIP array to each corresponding probe on an input (unenriched) array. These ratios were made more significant by applying a series of averaging and ranking steps to probes within a 400-bp sliding window; p73 binding sites were those that exhibited > 2.5-fold enrichment for at least 180 bp of consecutive probes (GenPathway FactorPath Protocol). The "negative peaks" approach was used to estimate error and calculate the false-discovery rate, as previously described (8).

The following software programs were used for statistical analyses, gene annotations, and determination of categorical enrichment as indicated: University of California Santa Cruz genome browser and tables (hg18; http://genome.ucsc.edu), Integrated Genome Browser (Affymetrix), NCBI DAVID, Kyoto Encyclopedia of Genes and Genomes (KEGG) (9), and WebGestalt (Bioinformatics Resource Center at Vanderbilt University, Nashville, TN) (10). De novo identification of enriched sequence motifs was performed using MEME (11). CEAS (*cis*-regulatory element annotation system) (12) was used for conservation analysis, annotation of functional elements, and identification of TRANSFAC- and JASPAR-enriched motifs. Briefly, ≈800 well-characterized eukaryotic motifs collected from TRANSFAC and JASPAR are in the CEAS database. The number of motifs present in p73-bound loci and in the whole genome were calculated, and those motifs that were significantly enriched in p73-bound loci with fold-change greater than two and *P* value from binomial test < 1E-10 were considered for further analysis (12).

Survival Analyses. A total of 134 patients in the Davicioni et al. cohort that had alveolar or embryonal rhabdomyosarcoma and a known survival time were included in survival analyses (7, 13). These tumors had been profiled using Affymetrix HG U133A arrays. Expression data were extracted from the Davicioni et al. dataset for 18 probes (corresponding to 17 genes) that are indicated in orange text in Fig. S4*C*; these are the direct p73 target genes from among all p73-regulated genes that clustered alveolar rhabdomyosarcomas by clinical outcome (alive vs. deceased). The relationship between this 17-gene p73 signature and overall clinical survival time was examined further using 10,000 resampling tests.

Expression data for each Affymetrix probe set were treated as the independent variable, and the Cox proportional hazard model was used for survival analyses. The number of significant probes with Wald *P* value ≤ 0.01 was saved as the observed number of significant probes. β (from the Cox model) and Wald statistics for each Affymetrix probe set were used along with expression data to build up a compound score for each patient. The compound score was used as the independent variable to perform overall survival analysis based on the Cox model. The compound score for patient *i* is defined as $\Sigma_j W_j \cdot X_{ij}$, where W_j = Wald statistic score for probe *j*, and $X_{ij} = \log_2$ probe *j* expression level for patient *i*. The Wald test *P* value was saved as the observed *P* value. For the resampling test, we randomly selected 18 probes without replacement among all possible Affymetrix probes in the array (22,283 probes), and repeated the above procedure of determining the number of significant probes, building up a compound score and calculating a Wald test *P* value. We repeated the resampling and survival analysis procedure 10,000 times, generating 10,000 resampling numbers of significant probes and Wald test *P* values, to confirm that our observed values were outside of the range of values that occur by chance. For alveolar tumors, only 0.18% of the 10,000 resampling *P* values were smaller than the observed *P* value. In contrast, for embryonal tumors, 73.5% of the 10,000 resampling *P* values were smaller than the observed *P* value and none of the probes were significant. Thus, the 18-probe p73 signature segregates alveolar rhabdomyosarcomas but not embryonal rhabdomyosarcomas by clinical outcome.

Next, we performed Kaplan-Meier analysis for the 64 patients with alveolar rhabdomyosarcoma in the cohort. For a given set of patients with compound scores, we divided the patients into two groups based on the median of the compound score. We plotted survival curves based on this grouping. The *P* value of the log-rank test based on this grouping is shown on the plot in Fig. 4*C*. Validation of the model was performed using the c-index, also indicated on the plot. The c-index is the probability of concordance between predicted and observed survival, with c = 0.5 for random predictions, and c = 1 for a perfectly discriminating model.

The multivariable Cox model was used to examine if the p73 signature score was independently prognostic for survival. The p73 signature score, stage, tumor size, age, and interaction effect between p73 signature score and stage were simultaneously included in the multivariable Cox model. The adjusted *P* values as well as the adjusted 95% confidence interval of the hazard ratios were reported (Table S3).

1. Rosenbluth JM, Mays DJ, Pino MF, Tang LJ, Pietenpol JA (2008) A gene signature-based approach identifies mTOR as a regulator of p73. *Mol Cell Biol* 28:5951–5964.
2. Mishra PJ, et al. (2008) Carcinoma-associated fibroblast-like differentiation of human mesenchymal stem cells. *Cancer Res* 68:4331–4339.
3. Perez CA, Ott J, Mays DJ, Pietenpol JA (2007) p63 consensus DNA-binding site: Identification, analysis and application into a p63M Halgorithm. *Oncogene* 26: 7363–7370.
4. Soutoglou E, Talianidis I (2002) Coordination of PIC assembly and chromatin remodeling during differentiation-induced gene activation. *Science* 295:1901–1904.
5. Ventura A, et al. (2004) Cre-lox-regulated conditional RNA interference from transgenes. *Proc Natl Acad Sci USA* 101:10380–10385.
6. Wachtel M, et al. (2004) Gene expression signatures identify rhabdomyosarcoma subtypes and detect a novel t(2;2)(q35;p23) translocation fusing PAX3 to NCOA1. *Cancer Res* 64:5539–5545.
7. Davicioni E, et al. (2006) Identification of a PAX-FKHR gene expression signature that defines molecular classes and determines the prognosis of alveolar rhabdomyosarcomas. *Cancer Res* 66:6936–6946.
8. Johnson WE, et al. (2006) Model-based analysis of tiling-arrays for ChIP-chip. *Proc Natl Acad Sci USA* 103:12457–12462.
9. Ogata H, Goto S, Fujibuchi W, Kanehisa M (1998) Computation with the KEGG pathway database. *Biosystems* 47:119–128.
10. Zhang B, Kirov S, Snoddy J (2005) WebGestalt: An integrated system for exploring gene sets in various biological contexts. *Nucleic Acids Res* 33(Web Server issue): W741–W748.
11. Bailey TL, Elkan C (1995) The value of prior knowledge in discovering motifs with MEME. *Proc Int Conf Intell Syst Mol Biol* 3:21–29.
12. Ji X, Li W, Song J, Wei L, Liu XS (2006) CEAS: *cis*-regulatory element annotation system. *Nucleic Acids Res* 34(Web Server issue):W551–W554.
13. Davicioni E, et al. (2009) Molecular classification of rhabdomyosarcoma—genotypic and phenotypic determinants of diagnosis: a report from the Children's Oncology Group. *Am J Pathol* 174:550–564.

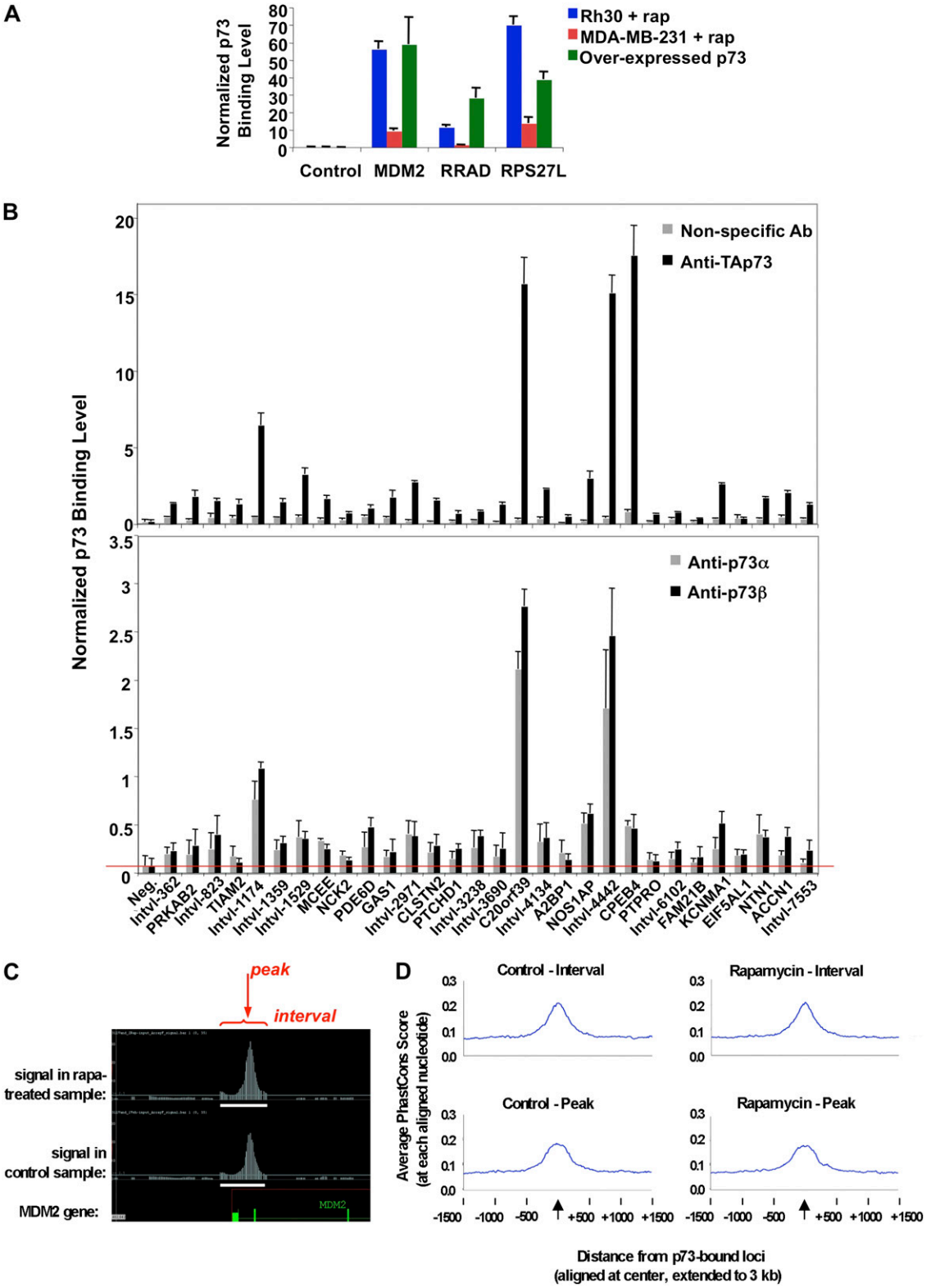

Fig. S1. Verification of p73 binding by qRT-PCR and conservation analysis. (*A*) ChIP-qPCR was performed to assess p73 occupancy at genomic regions in *MDM2*, *RRAD*, and *RPS27L* promoters in p53-mutant Rh30 or MDA-MB-231 cells treated with 40 nM rapamycin (rap) for 24 h. To facilitate comparison across cell lines, ChIP-qPCR was also performed in H1299 lung carcinoma cells transduced with an adenovirus that expresses high levels of p73. Binding levels were normalized to input; "Control" represents a negative-control region. Error bars represent SD from triplicate analyses. (*B*) To confirm the ChIP-on-Chip results, p73 occupancy was remeasured using different antibodies and methodology. Thirty loci were chosen randomly from among all p73-bound regions. The gene nearest each genomic interval is indicated when located within 10 kb, otherwise a generic interval number ("Intvl-#") is given. (*Upper*) Nonspecific antibody (rabbit IgG) and the A300-126A anti-TAp73 (rabbit antibody that was used for ChIP-on-Chip) are compared. (*Lower*) Binding of p73 was confirmed by immunoprecipitating either

Legend continued on following page

p73α or p73β. These immunoprecipitations were performed using sonicated lysates prepared from formaldehyde cross-linked Rh30 cells, and by PCR-amplifying associated DNA fragments using primers flanking each of the 30 sites. Of note, the two antibodies used preferentially recognize either p73α or p73β, suggesting that both p73 isoforms bind to the same sites, either directly or through hetero-dimerization with the other p73 isoform. Although we cannot formally distinguish between hetero-oligomers and mixed populations of TAp73α and TAp73β homo-dimer-DNA complexes, each p73 binding site as measured by ChIP-on-Chip is likely to reflect genuine binding by both TAp73α and TAp73β. (*C*) The *MDM2* gene is depicted using the Integrated Genome Browser to demonstrate two dimensions of p73 occupancy. The "interval" is the region across which p73 binding exceeds threshold. The "peak" is the location in the interval with the highest p73 binding level. (*D*) Sequence conservation was determined using phastCons scores from the University of California Santa Cruz GoldenPath genome resource in both control and rapamycin-treated samples. The conservation of broad p73-bound intervals and more sharply defined peaks was assessed. Regions were extended to 3 kb and aligned at their centers, and an average conservation score was calculated at each aligned nucleotide. Conservation is higher at p73-bound regions (center of each plot), compared with genomic background (at both ends of each plot).

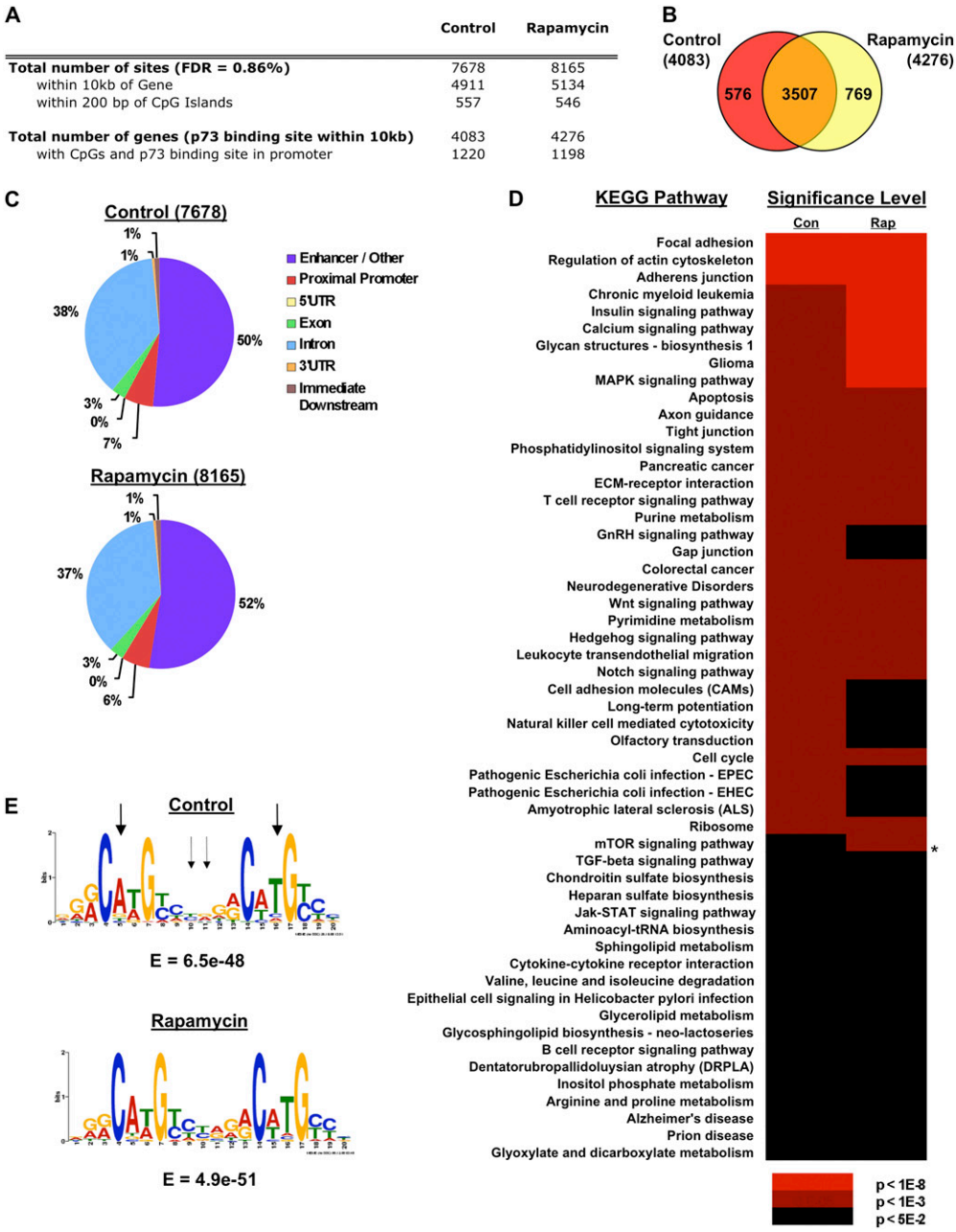

Fig. S2. The regulatory regions of genes are bound by p73 at a specific consensus binding motif. (*A*) The total number of p73 binding sites (false-discovery rate, 0.86%), the number of sites within 10 kb of genes, and the number of sites within 200 bp of CpG islands are listed for control and rapamycin-treated samples. The total number of genes within 10 kb of a p73 binding site, and the number with CpG islands and p73 binding sites in promoter regions (from −7,500 to +2,500 of gene start) are also indicated. (*B*) Schematic showing that ∼86% of p73-bound genes in control samples are also bound by p73 in rapamycin-treated samples. (*C*) We determined the percentages of p73 binding sites that reside in proximal promoters (1 kb upstream from 5′ gene start), immediate downstream regions (1 kb downstream from 3′ gene end), 5′ UTRs, 3′ UTRs, coding exons, introns, and enhancers/other (more than 1 kb from any gene), based on National Center for Biotechnology Information Reference Sequences (1). Pie charts depict the percentage of p73 binding sites that reside in the indicated functional elements in control and rapamycin-treated samples. The "enhancers/other" category includes experimentally validated enhancers from the VISTA Enhancer Browser (http://enhancer.lbl.gov/), as well as sites of unknown function that are more than 1 kb from a gene. (*D*) Kyoto Encyclopedia of Genes and Genomes database signaling pathways that are enriched among genes within 10 kb of p73-binding sites are shown for control (con) and rapamycin-treated samples (rap). Significance is indicated by color, based on *P* values from hypergeometric tests. The mTOR pathway is marked with " * ". (*E*) Motifs identified de novo from the top 50 p73-bound sequences in control and rapamycin-treated samples are shown. These motifs were validated in the top 500 p73-bound sequences in groups of 50 in control samples and in all p73 binding sites on chromosome 22, giving the same consensus binding sequence. Arrows indicate similarities in the motifs of p63 and p73 that are more degenerate than p53. These results suggest that, like p53 and p63, p73 is capable of binding sequences that deviate from its consensus motif (2, 3). The height of each nucleotide indicates its relative frequency at that position in the motif. The probability of identifying an equally well-conserved pattern in random sequences (E-value) is also indicated for each motif. We validated the p73 consensus binding sequence by performing the Systematic Evolution of Ligands by Exponential enrichment technique (SELEX), in which the affinity of p73 for randomly generated oligonucleotide motifs is measured in vitro. SELEX did identify the p73 consensus binding sequence from a pool of random sequences.

1. Ji X, Li W, Song J, Wei L, Liu XS (2006) CEAS: *cis*-regulatory element annotation system. *Nucleic Acids Res* 34(Web Server issue):W551–W554.
2. Yang A, et al. (2006) Relationships between p63 binding, DNA sequence, transcription activity, and biological function in human cells. *Mol Cell* 24:593–602.
3. Wei CL, et al. (2006) A global map of p53 transcription-factor binding sites in the human genome. *Cell* 124:207–219.

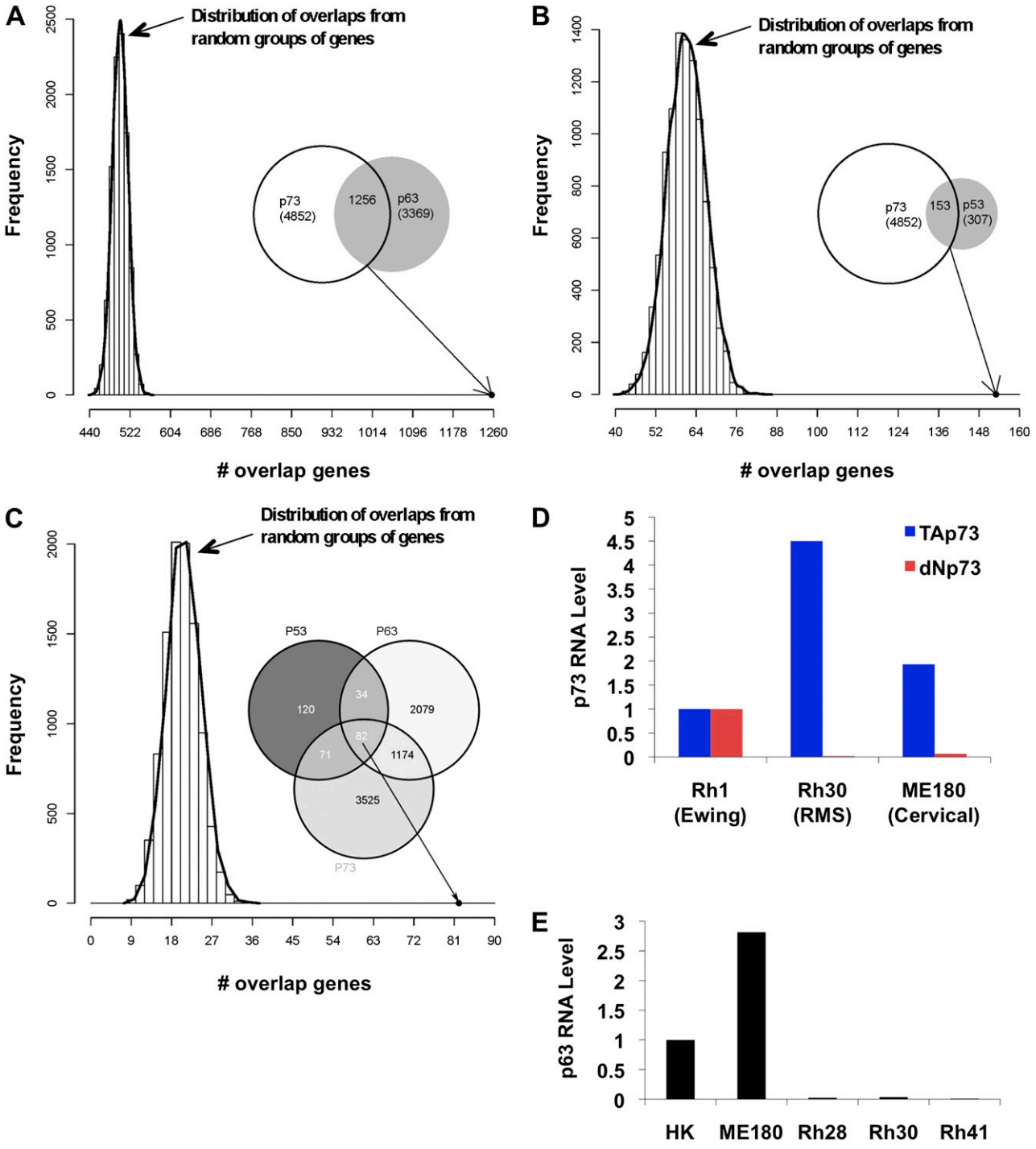

Fig. S3. Regulation of common and distinct sets of genes by p53, p63, and p73. The observed overlap between p73-bound genes and (*A*) p63-bound genes (from ref. 1) or (*B*) p53-bound genes (from ref. 2) is compared with the overlaps of 10,000 random groups of equivalent size. None of the random overlaps has a larger overlap than the observed data ($P < 0.0001$). (*C*) The p53, p63, and p73-bound genes are compared with 10,000 random groups of equivalent size as above. See *SI Appendix*, Datasets S1A, S1B, and S1C for the full list of genes in each intersection. (*D*) RNA was harvested from the indicated Ewing's sarcoma (Rh1), rhabdomyosarcoma (RMS, Rh30), and cervical cancer (ME180) cell lines. TAp73 and ΔNp73 (dNp73) RNA levels were determined using qRT-PCR, and are shown relative to levels in the Rh1 cell line. (*E*) RNA was harvested from the indicated cells and cell lines: HK (human keratinocytes), ME180 (cervical cancer cell line), Rh28, Rh30, and Rh41 (rhabdomyosarcoma cell lines). Quantitative RT-PCR was performed to determine p63 RNA levels using GAPDH as a control.

1. Yang A, et al. (2006) Relationships between p63 binding, DNA sequence, transcription activity, and biological function in human cells. *Mol Cell* 24:593–602.
2. Wei CL, et al. (2006) A global map of p53 transcription-factor binding sites in the human genome. *Cell* 124:207–219.

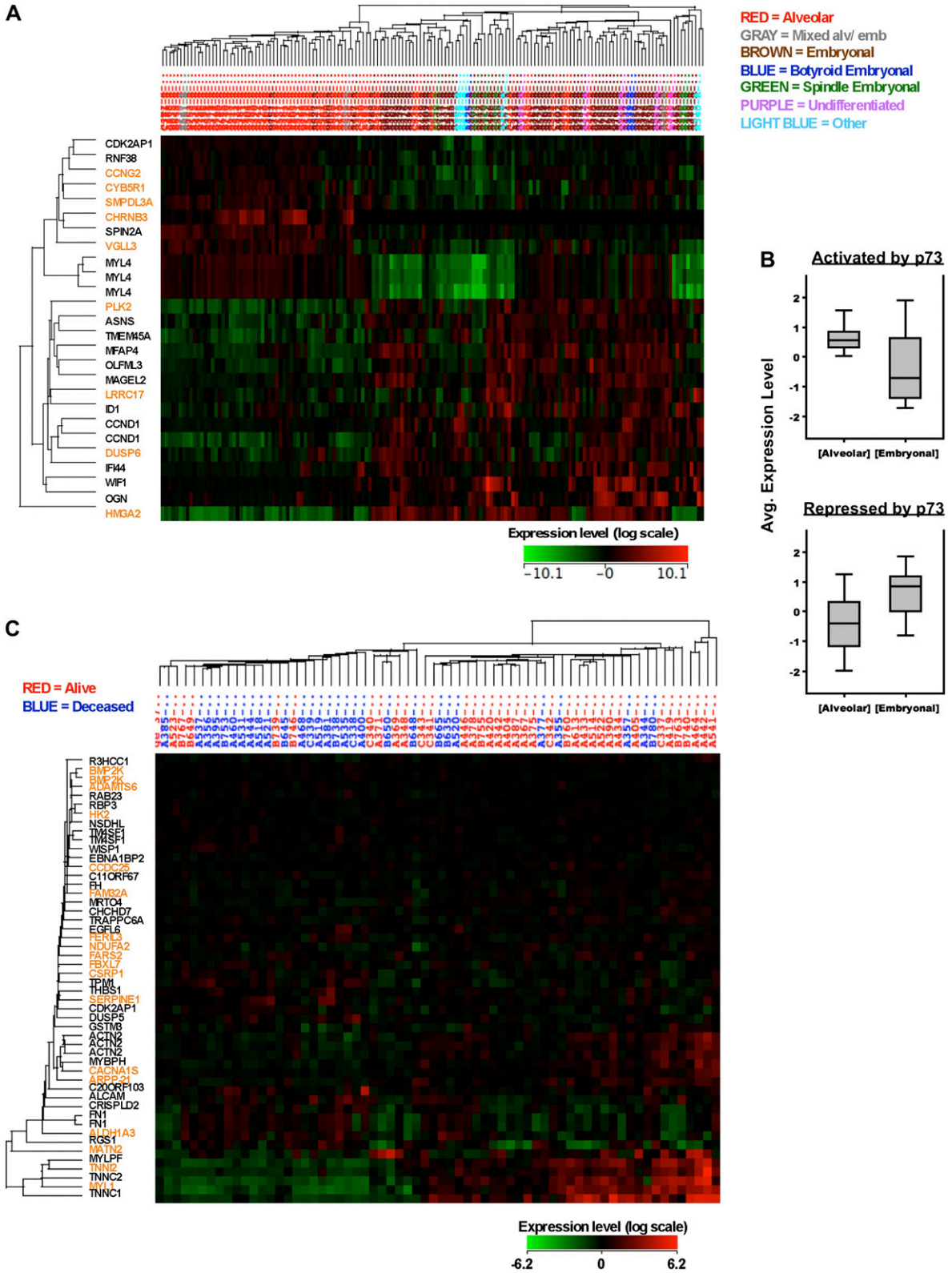

Fig. S4. Differential expression of the p73 signature in an independent cohort of alveolar and embryonal rhabdomyosarcomas. The mTOR-p73 gene signature was assessed using a second publicly available data set, in which 139 rhabdomyosarcoma tumors were profiled by microarray (1). (*A*) Hierarchical clustering demonstrates that the mTOR-p73 gene signature segregates tumors into two classes, corresponding to the clinical subtypes alveolar and embryonal. (Botryoid and spindle tumors are subtypes of embryonal tumors. Tumors marked as "other" could not be classified.) Those p73-regulated genes that were most significantly associated with alveolar rhabdomyosarcoma (ARMS) are shown. These 23 genes exhibit significant differential expression in the two subtypes (multiple testing-corrected P value < 0.001, fold-change > 2). Direct p73 target genes are highlighted in orange text. (*B*) Genes positively regulated $> 50\%$ by p73 and genes negatively regulated $> 50\%$ by p73 were analyzed in alveolar and embryonal rhabdomyosarcoma (ERMS) subtypes, demonstrating opposing gene expression patterns in these two tumor subtypes. As a control, we examined the ability of all genes (unfiltered) to segregate rhabdomyosarcomas and

Legend continued on following page

found that ARMS and ERMS were not segregated in either cohort as they were by p73-regulated genes. Similarly, a p53 gene signature that is associated with p53 mutation status was unable to segregate ARMS and ERMS tumors (2). Of note, p73 RNA expression levels in alveolar and embryonal tumor groups varied by only 2 to 4%. Cofactors involved in muscle development from Fig. 2*A* that exhibited greater than twofold differences in expression between alveolar and embryonal subtypes are Myf, MyoD, Tead1, and Zeb1. (*C*) ARMS microarray data were separated from the Davicioni et al. dataset and annotated by 5-y survival outcome (1). In this cohort we could identify genes in our p73 signature that correlated with 5-y survival after treatment for ARMS. The probes in the p73 signature that exhibited the most significant association with patient outcome (by Benjamini-Hochberg false-discovery rate *t* test) are shown by gene. Hierarchical clustering was performed with these probes, leading to partial segregation of tumors from alive and deceased outcomes. Genes present in the p73 ChIP-on-Chip dataset are indicated in orange text.

1. Davicioni E, et al. (2006) Identification of a PAX-FKHR gene expression signature that defines molecular classes and determines the prognosis of alveolar rhabdomyosarcomas. *Cancer Res* 66:6936–6946.
2. Miller LD, et al. (2005) An expression signature for p53 status in human breast cancer predicts mutation status, transcriptional effects, and patient survival. *Proc Natl Acad Sci USA* 102: 13550–13555.

Table S1. MicroRNA promoters bound by p73

Chrom no.	Promoter start	Promoter end	miRNA	p73 binding level*	Nearby genes†
5	59100080	59100279	miR-582	3.5	*PDE4E*
10	91395210	91395409	miR-107	7.6	*PANK1*
12	61282697	61282896	let-7i	3.7	*C12orf61*
12	93540063	93541288	miR-492	11.9	*TMCC3*
16	14309749	14312532	miR-365–1	3.7	*LOC10019781*
16	15643093	15645825	miR-484	18.9	*KIAA0430*, *NDE1*
17	76753312	76755359	miR-338	2.8	*NM_207389*, *KIAA0641*
17	76753312	76755359	miR-657	2.8	*NM_207389*, *KIAA0641*

*From the ChIp-on-Chip Dataset.
†Within 10 kb of the miRNA.

Table S2. Muscle-related Biocarta pathways enriched among p73-bound genes ($P < 0.05$)

Muscle-related pathways	Enrichment ratio*
Skeletal muscle hypertrophy is regulated via AKT/mTOR pathway	2.1
CUTL1	
IGF1	
IGF1R	
PPP2R4	
RPS6KB1	
EIF2B4	
Control of skeletal myogenesis by HDAC and calcium/calmodulin-dependent kinase (CaMK)	2.4
HDAC5	
CABIN1	
IGF1	
IGF1R	
INSR	
PPP3CA	
Actions of nitric oxide in the heart	2.6
CRAT	
PDE3B	
ACTA1	
BDKRB2	
TNNI2	
CAV1	
NFAT and hypertrophy of the heart (transcription in the broken heart)	2.0
CSNK1A1	
HBEGF	
GATA4	
IGF1	
LIF	
PPP3CA	
MAP2K1	
ACTA1	
RPS6KB1	
CAMK4	
Role of EGF receptor transactivation by GPCRs in cardiac hypertrophy	3.3
EGF	
EGFR	
FOS	
RHOA	
NFKB1	
PRKCA	
ADAM12	
ALK in cardiac myocytes	2.7
GATA4	
SMAD1	
SMAD5	
NPPB	
BMP5	
BMP7	
BMPR2	
TGFBR1	
TGFBR2	
TGFBR3	
AXIN1	
ACVR1	

$P < 0.05$ calculated by hypergeometric test.
*Number of observed genes in category/number of genes expected by chance.

Table S3. Multiple Cox model of rhabdomyosarcomas and compound score of p73 gene signature

Tumor type	Coefficient	*z*-Score	*P* value	Lower 95% CI	Upper 95% CI
Alveolar					
p73 compound score	0.052	2.490	0.013*	1.011	1.097
Stage I/II/III versus IV	−7.132	−1.859	0.063	0.000	1.472
Tumor size> 5 cm	1.454	1.336	0.180	0.507	36.126
Patient age	−0.053	−0.616	0.540	0.801	1.123
Interaction: compound score and stage	−0.042	−1.671	0.095†	0.912	1.007
Embryonal					
p73 compound score	−0.007	−0.764	0.44‡	0.974	1.012
Stage I/II/III versus IV	4.099	1.506	0.130	0.290	12,509.282
Tumor size> 5 cm	0.028	0.042	0.970	0.276	3.825
Patient age	0.046	0.723	0.470	0.924	1.187
Interaction: compound score and stage	0.047	2.347	0.019	1.008	1.090

*Indicates p73 signature is significant when corrected for three additional variables (stage, size, and age).
†Indicates no interaction between p73 signature and stage.
‡Indicates p73 signature is not significant when corrected for three variables (stage, size, and age) in embryonal tumor subset.

Other Supporting Information Files

SI Appendix (XLS)